

# Stirring Strongly Coupled Plasma

---

Kazem Bitaghsir Fadafan<sup>1</sup>, Hong Liu<sup>2</sup>, Krishna Rajagopal<sup>2</sup> and Urs Achim Wiedemann<sup>3</sup>

<sup>1</sup>*Physics Department, Shahrood University of Technology, Shahrood, Iran*

<sup>2</sup>*Center for Theoretical Physics, MIT, Cambridge, MA 02139, USA*

<sup>3</sup>*Department of Physics, CERN, Theory Division, CH-1211 Geneva 23*

*E-mail addresses:* bitaghsir@shahroodut.ac.ir, hong\_liu@mit.edu, krishna@ctp.mit.edu, Urs.Wiedemann@cern.ch

**ABSTRACT:** We determine the energy it takes to move a test quark along a circle of radius  $L$  with angular frequency  $\omega$  through the strongly coupled plasma of  $\mathcal{N} = 4$  supersymmetric Yang-Mills (SYM) theory. We find that for most values of  $L$  and  $\omega$  the energy deposited by stirring the plasma in this way is governed either by the drag force acting on a test quark moving through the plasma in a straight line with speed  $v = L\omega$  or by the energy radiated by a quark in circular motion in the absence of any plasma, whichever is larger. There is a continuous crossover from the drag-dominated regime ( $\omega \lesssim \pi T(1-v^2)^{3/4}$ , meaning  $\omega \lesssim \pi T$  and  $L$  small enough) to the radiation-dominated regime ( $\omega \gtrsim \pi T(1-v^2)^{3/4}$ ). In the crossover regime we find evidence for significant destructive interference between energy loss due to drag and that due to radiation as if in vacuum. The rotating quark thus serves as a model system in which the relative strength of, and interplay between, two different mechanisms of parton energy loss is accessible via a controlled classical gravity calculation. We close by speculating on the implications of our results for a quark that is moving through the plasma in a straight line while decelerating, although in this case the classical calculation breaks down at the same value of the deceleration at which the radiation-dominated regime sets in.

**KEYWORDS:** AdS/CFT correspondence, Thermal Field Theory.

---

## Contents

<b>1. Introduction</b>	<b>1</b>
<b>2. A Rotating Quark and a Spiralling String</b>	<b>3</b>
2.1 Formulation of the problem	3
2.2 One special point on the spiralling string	7
2.3 Radial dependence of the spiralling string	8
2.4 Angular dependence of the spiralling string	10
2.5 Rotating quark in vacuum	12
<b>3. Energy Lost by a Rotating Quark</b>	<b>13</b>
3.1 General and numerical results	13
3.2 Energy loss in two limits: linear drag and vacuum radiation	15
3.3 Where the calculation breaks down	20
<b>4. Speculations About Linear Motion</b>	<b>21</b>

---

## 1. Introduction

Parton energy loss in hot plasmas has been studied intensely in recent years [1]. Experimentally, the phenomenon can be accessed by measuring the remnants of jets that are quenched by the hot and dense matter produced in relativistic heavy ion collisions at RHIC [2] or at the LHC [3]. The modification of quenched jets provide one of the best tools for constraining properties of the matter produced in heavy ion collisions. Furthermore, the energy lost by the quenched jet provides a localized perturbation of the surrounding matter that is expected to give rise to characteristic collective phenomena such as cone-like momentum flow patterns [4]. These are searched for in the data.

In the high projectile-energy limit, the energy loss of a relativistic parton is dominated by gluon bremsstrahlung and calculations based upon perturbative QCD are reliable [1]. These calculations describe the destructive interference between the vacuum radiation of a virtual parton and the additional QCD bremsstrahlung radiation that is sensitive to the acceleration of the colored projectile moving through the medium [1]. At lower projectile energies other mechanisms including collisional energy loss via elastic interactions may contribute to parton energy loss. And, even in the high projectile-energy limit the interactions of the partonic jet fragments with the medium involve small momentum transfers, of order the temperature if the medium is in equilibrium, and are thus expected to be governed by a nonperturbatively strong coupling constant. However, strong

coupling calculations of dynamic processes in QCD are notoriously difficult. This has motivated parton energy loss calculations in a class of supersymmetric theories, for which the AdS/CFT correspondence [5] provides powerful techniques for doing calculations at strong coupling. Two different strategies have been pursued:

In one approach, one identifies the nonperturbative properties of the strongly coupled medium that must be put into the otherwise perturbative QCD energy loss calculations in terms of a light-like Wilson loop [6], which is then calculated with the help of the AdS/CFT correspondence [7, 8]. The range of validity of this calculation is limited to very energetic partonic projectiles, where the dominant energy loss mechanism is indeed radiative and the perturbative calculation (with a nonperturbative input that plays the same logical role that parton distribution functions do in deep inelastic scattering) is valid.

In the other approach, one assumes that the initial production of hard partons is perturbative<sup>1</sup> but then treats the parton energy loss process as if interactions at all relevant scales are nonperturbatively strong and therefore formulates the entire energy loss calculation in the gravity dual of a strongly coupled supersymmetric gauge theory. The simplest problem to consider is the force required to move a projectile through the plasma at some constant velocity [11, 12]. If the projectile velocity is sufficiently small, the gravity description is in terms of a classical string trailing “down” into the five-dimensional spacetime behind the quark moving along the four-dimensional boundary. This classical calculation breaks down at high enough velocities because the force required to maintain the quark at constant velocity becomes large enough that quark antiquark pair production is unsuppressed [13]. In the velocity regime in which this calculation is reliable, it yields the result that the force required to keep the quark moving is proportional to the quark momentum, meaning that energy loss occurs via drag [11, 12]. Quantum fluctuations of the string trailing behind the quark translate into fluctuations in the momentum of the quark [14, 15, 13]. It is an open question, however, how to make a quantitative translation from these results to the physically relevant setting in which there is no external force acting on the energetic colored projectile, which is therefore decelerating. This deceleration opens the possibility of additional mechanisms of parton energy loss, since at least in vacuum we know that it would lead to radiation. And, it raises the possibility of interference between medium-induced energy loss (in this case drag) and deceleration-induced energy loss. Motivated by these questions, which remain open, we have found a different simple problem to consider in which, within the regime of validity of the classical trailing string calculation, we find that energy loss can either be dominated by drag or can be as if the quark were radiating in vacuum, and behaves as if energy loss via these two mechanisms interfere destructively.

In the present work, we determine the energy needed to move a heavy test quark along a circle of radius  $L$  with angular frequency  $\omega$  through the strongly coupled plasma of  $\mathcal{N} = 4$  supersymmetric Yang-Mills (SYM) theory. We are interested in this problem since it provides a novel perspective on several of the open questions mentioned above. Because in vacuum a rotating colored particle would emit synchrotron radiation, studying a particle moving in a circle with constant angular velocity through a strongly coupled plasma is well suited to studying the relative strength of, and interplay between, radiation and medium-induced energy loss, as a function of  $\omega$  and  $L$ . It

---

<sup>1</sup>This must be the case since if the initial hard scattering were also described within the strongly coupled theory, one would observe hedgehog-like hard-scattering events rather than the jet-like events seen at RHIC [9, 10].

will also allow us to compare radiation in medium and in vacuum. Also, in contrast to linear motion with acceleration, the case of rotation at constant angular velocity can be formulated as an essentially time-independent problem even though it includes acceleration. Finally, stirring a strongly coupled plasma by a rotating quark is a well-localized source of plasma perturbations whose propagation and dissipation is described in the dual gravity theory by the trailing string. We leave the translation from the trailing string description to the corresponding stress-energy tensor describing the disturbance of the gauge theory plasma to future work.

Our paper is organized as follows: In Section 2, we calculate the shape of the trailing string spiralling below the quark at its endpoint, which is being pulled with constant angular velocity along a circle within strongly coupled  $\mathcal{N} = 4$  SYM plasma. This is the gravity dual of a rotating heavy quark and the disturbance that the rotating quark creates by depositing energy in the plasma. In Section 3, we determine the corresponding energy loss and compare the result to expectations if the energy loss were due to acceleration-induced radiation in the absence of any medium and to expectations if the energy loss were due to drag in the absence of any acceleration. We find that in regimes in which one of these is much larger than the other, the larger one is a good approximation to our result. Where both expectations are comparable, our result is less than their sum, indicating destructive interference. By comparing the shape of the trailing string in medium to that in vacuum, we show that even in the regime in which the energy loss behaves precisely as if the rotating quark were emitting synchrotron radiation in vacuum, the disturbance of the plasma due to the deposited energy is not the same as the radiation pattern for synchrotron radiation in vacuum. In Section 4 we return to the case of linear motion, which motivated our investigation. We show that the classical calculation breaks down just at the velocity at which energy loss due to deceleration-induced radiation becomes comparable to that due to drag. This is in contrast to the case of circular motion, where we find a wide range of parameters  $\omega$  and  $L$  where the classical calculation is reliable and acceleration-induced radiation dominates over drag. We nevertheless close by using our results to speculate about the role of radiation for the case of linear motion.

## 2. A Rotating Quark and a Spiralling String

### 2.1 Formulation of the problem

We shall consider a heavy test quark moving through the strongly coupled plasma of  $\mathcal{N} = 4$  SYM with temperature  $T$ . We assume that there is some external agent exerting a suitable force on the quark such that it moves along a circle of radius  $L$  at a constant angular frequency  $\omega$ . The quark has a constant speed

$$v = L\omega , \tag{2.1}$$

and it has a constant acceleration perpendicular to its direction of motion,

$$a = \omega v = \omega^2 L . \tag{2.2}$$

We wish to compute  $dE/dt$ , the energy lost per unit time by the quark as it stirs the plasma.  $dE/dt$  is the energy expended by the external agent moving the quark, and it is also the energy dumped into the plasma that is being stirred. We shall do the computation using the gravity dual of  $\mathcal{N} = 4$

SYM, following the basic logic first developed in the study of a test quark being moved along a straight line at constant speed through the plasma [11, 12]. Although we do not know of a physical realization of the problem that we solve, it is instructive because, as we shall see, it exhibits a crossover between a regime in which  $dE/dt$  is dominated by the drag force experienced by a quark moving in a straight line with speed  $v$  to a regime in which  $dE/dt$  is dominated by the radiation that arises by virtue of the acceleration  $a$ .

$\mathcal{N} = 4$  SYM theory is a supersymmetric gauge theory characterized by two parameters: the rank of the gauge group  $N_c$  and the 't Hooft coupling  $\lambda = g_{\text{YM}}^2 N_c$ , where  $g_{\text{YM}}$  is the gauge coupling. The theory is conformal, meaning that  $\lambda$  is a parameter that we can choose. If we choose  $\lambda$  large, at  $T \neq 0$  this theory describes a strongly coupled plasma. According to the AdS/CFT correspondence [5], this gauge theory is equivalent to Type IIB string theory in  $\text{AdS}_5 \times S_5$  spacetime, with the curvature radius  $R$  of the Anti deSitter (AdS) space and the string tension  $1/(2\pi\alpha')$  related to the 't Hooft coupling by

$$\sqrt{\lambda} = \frac{R^2}{\alpha'} . \quad (2.3)$$

The gauge theory can be thought of as living on the boundary of  $\text{AdS}_5$ . If we take  $N_c \rightarrow \infty$  at fixed  $\lambda$  and then take  $\lambda$  large,  $\mathcal{N} = 4$  SYM theory has a gravity dual: it is described by classical supergravity on  $\text{AdS}_5 \times S_5$ . Nonzero temperature  $T$  in the gauge theory corresponds to replacing the  $\text{AdS}_5$  spacetime in the gravity dual by a 5-dimensional AdS black hole, with the metric

$$ds^2 = -f(\tilde{u}) dt^2 + \frac{\tilde{u}^2}{R^2} (d\tilde{\rho}^2 + \tilde{\rho}^2 d\varphi^2 + dx_3^2) + \frac{d\tilde{u}^2}{f(\tilde{u})} , \quad (2.4)$$

$$f(\tilde{u}) \equiv \frac{\tilde{u}^2}{R^2} \left( 1 - \frac{\tilde{u}_h^4}{\tilde{u}^4} \right) . \quad (2.5)$$

Here, the bulk coordinate in the 5th dimension is  $\tilde{u}$  and  $\tilde{u}_h$  is the Schwarzschild radius at which we find the horizon of the black hole. The temperature in the gauge theory is equal to the Hawking temperature of the AdS black hole in the gravity dual, namely

$$T = \frac{\tilde{u}_h}{\pi R^2} . \quad (2.6)$$

In (2.4), we have written two of the three spatial dimensions using radial coordinates  $(\tilde{\rho}, \varphi)$ , with the third spatial coordinate being  $x_3$ . The coordinates  $\tilde{u}$  and  $\tilde{\rho}$  have dimensions of length; we shall soon replace them by dimensionless coordinates, and drop the tildes.

In the gravity dual, a heavy test quark corresponds to an open string with one end-point on a D3-brane at  $\tilde{u} = \infty$ . The string hangs down into the bulk, extending towards the black hole horizon at  $\tilde{u} = \tilde{u}_h$ . In order to use the gravity dual description of  $\mathcal{N} = 4$  SYM to determine  $dE/dt$  for a quark moving in a circle, we must first (in this Section) find the worldsheet of the string spiralling downward from the quark moving on a circle at  $u = \infty$  and then (in the next Section) calculate the energy flowing down the string. We choose to parameterize the two dimensional worldsheet of the rotating string  $X^\mu(\tau, \sigma)$  according to

$$X^\mu(\tau, \sigma) = (t = \tau, \tilde{\rho} = \tilde{\rho}(\tilde{u}), \varphi = \omega\tau + \theta(\tilde{u}), x_3 = 0, \tilde{u} = \sigma) . \quad (2.7)$$

Here and throughout, indices  $\mu$  and  $\nu$  run over five dimensions,  $\mu, \nu \in (t, \tilde{\rho}, \varphi, x_3, \tilde{u})$ . Below, indices  $a, b$  run over the two dimensions of the worldsheet,  $a, b \in (\sigma, \tau)$ . In order to describe the rotating quark that we wish to analyze, the end-point of the string on the D3-brane must satisfy the boundary conditions

$$\begin{aligned}\tilde{\rho}(\infty) &= L, \\ \theta(\infty) &= 0.\end{aligned}\tag{2.8}$$

In writing the parameterization (2.7), we have made use of the fact that the quark is in circular motion at a constant angular velocity, and has been moving in this way for all time. The entire time-dependence of the string therefore consists of a global rotation with the azimuthal angle  $\phi$  increasing with time according to  $\phi(\tau) = \omega\tau$  plus a  $\tau$ -independent, but  $\tilde{u}$ -dependent, function. This function  $\theta(\tilde{u})$ , together with the function  $\tilde{\rho}(\tilde{u})$  that specifies how the radius of the string depends on  $\tilde{u}$ , provide a complete specification of the shape of the spiralling string dangling down from the rotating quark. In order to visualize this set-up, it may be helpful to look at the example solution in Fig. 2.

We find explicit solutions  $\theta(\tilde{u})$  and  $\tilde{\rho}(\tilde{u})$  for the shape of the spiralling string by minimizing the Nambu-Goto action

$$S = -\frac{1}{2\pi\alpha'} \int d\tau d\sigma \sqrt{-\det g_{ab}} \equiv -\frac{1}{2\pi\alpha'} \int d\tau d\sigma \mathcal{L},\tag{2.9}$$

where

$$g_{ab} \equiv G_{\mu\nu} \partial_a X^\mu \partial_b X^\nu\tag{2.10}$$

is the induced metric on the worldsheet and  $G_{\mu\nu}$  is the spacetime metric (2.4). We shall find it convenient to describe the shape of the string with the dimensionless variables

$$u \equiv \frac{\tilde{u}}{\tilde{u}_h},\tag{2.11}$$

$$\rho \equiv \frac{\tilde{u}_h}{R^2} \tilde{\rho},\tag{2.12}$$

and specify the motion of the quark with the dimensionless parameters

$$\ell \equiv \frac{\tilde{u}_h}{R^2} L = L\pi T,\tag{2.13}$$

$$\mathbf{w} \equiv \frac{R^2}{\tilde{u}_h} \omega = \frac{\omega}{\pi T}.\tag{2.14}$$

Note that

$$v = L\omega = \ell \mathbf{w}\tag{2.15}$$

and note that the dimensionless acceleration of the quark at  $u = \infty$  is given by

$$\mathbf{a} = \mathbf{w}v = \mathbf{w}^2 \ell = \frac{a}{\pi T}.\tag{2.16}$$

The Lagrangian now takes the form

$$\mathcal{L} = \sqrt{(u^4 - \rho^2 \mathbf{w}^2 u^4 - 1) \left( \rho'^2 + \frac{1}{u^4 - 1} \right) + \rho^2 (u^4 - 1) \theta'^2}. \quad (2.17)$$

Here, the prime denotes a derivative with respect to the dimensionless bulk variable  $u$ , e.g.  $\rho' \equiv \partial\rho/\partial u$ . We then obtain the equations of motion

$$\partial_u \frac{\partial \mathcal{L}}{\partial \rho'} - \frac{\partial \mathcal{L}}{\partial \rho} = 0, \quad (2.18)$$

$$\partial_u \frac{\partial \mathcal{L}}{\partial \theta'} = 0 \quad (2.19)$$

from the Lagrangian (2.17). These are the equations that determine  $\rho(u)$  and  $\theta(u)$  and hence the shape of the spiralling string trailing below the rotating quark.

To solve the equations of motion (2.18), (2.19), we first focus on the angular dependence. The Lagrangian depends on  $\theta'$  but not on  $\theta$ , so there is a constant of the motion that we shall define as

$$\Pi \equiv -\frac{\partial \mathcal{L}}{\partial \theta'} = \frac{\theta' \rho^2 (u^4 - 1)}{\mathcal{L}}. \quad (2.20)$$

$\Pi$  will play a central role in our analysis. We shall see that for a given  $\mathbf{w}$  the spiralling string solutions can be specified either by giving the radius  $\ell$  of the motion of the quark at  $u = \infty$  or by giving  $\Pi$ . And, we shall see in Section 3 that the energy lost to the medium by the rotating quark is proportional to  $\Pi$ . Starting from (2.20), we can solve for  $\theta'(u)$  as a function of  $\rho(u)$ , obtaining

$$\theta'^2 = \frac{\Pi^2 (u^4 - \rho^2 \mathbf{w}^2 u^4 - 1) \left( \rho'^2 + \frac{1}{u^4 - 1} \right)}{\rho^2 (u^4 - 1) [\rho^2 (u^4 - 1) - \Pi^2]}. \quad (2.21)$$

We now see that we can use (2.21) to eliminate  $\theta'^2$  from (2.18), obtaining an equation of motion for  $\rho(u)$  in which the  $\theta$ -dependence manifests itself only through the presence of the constant  $\Pi$ . This equation can be written in the form

$$\rho'' + \frac{2u^3 \rho \rho' - 1}{\rho^2 (u^4 - 1) - \Pi^2} \rho (\rho'^2 (u^4 - 1) + 1) + \frac{2u^3 \rho \rho' (1 - \rho^2 \mathbf{w}^2 + \rho^2 \rho'^2 \mathbf{w}^2) + \rho'^2 (u^4 - 1) + 1}{(1 - \rho^2 \mathbf{w}^2) \rho u^4 - \rho} = 0. \quad (2.22)$$

After first solving the differential equation (2.22) to obtain  $\rho(u)$ , we will then be able to integrate (2.21) to obtain  $\theta(u)$ .

We note that for  $\Pi = 0$ , the angular equation of motion is trivial,  $\theta'(u) = 0$ , and the radial equation of motion (2.22) allows for another set of physical solutions with any radius  $\ell < 1/\mathbf{w}$ . These solutions have been studied as a model of rotating mesons [16, 17, 18]. Their radial shape  $\rho(u)$  decreases with decreasing  $u$ , reaches a turning point where  $\rho(u_{\text{turn}}) = 0$ ,  $\rho'(u_{\text{turn}}) = 0$ , and then rises back to  $u = \infty$ , which is reached on the same circle with radius  $\ell$  at  $\theta_{\text{end}} = \theta_{\text{start}} + \pi$ . These mesonic string configurations do not experience any energy loss within the supergravity approximation. In the present work, we focus solely on spiralling string solutions with  $\Pi \neq 0$ , noting from (2.21) that no solutions that pass through a turning point with  $\rho = 0$  can exist if  $\Pi \neq 0$ .

## 2.2 One special point on the spiralling string

Before implementing the procedure that we have just described for finding the string worldsheet, it is helpful to first consider some general properties of the solutions that we are looking for. The rotating quark corresponds to a string which starts at the boundary  $u = \infty$  at a radius  $\rho(\infty) = \ell$ , and which hangs down into the bulk and approaches the black hole horizon. At the boundary, the numerator in (2.21) is positive because  $v = \ell \mathbf{w} < 1$ . At each position  $u$  in the bulk, the string will be subject to a centrifugal force. This implies that  $\rho(u) > \ell$  for all values of  $u < \infty$  in the bulk. Consequently, once the string reaches the horizon,  $u = 1$ , the factor  $(u^4 - \rho^2 \mathbf{w}^2 u^4 - 1)$  in the numerator in (2.21) must have changed sign and become negative. The numerator changes sign at the point  $(u_c, \rho_c)$  where the string solution crosses the curve

$$\rho_{\text{light}}(u, \mathbf{w}) = \frac{1}{\mathbf{w}} \sqrt{1 - \frac{1}{u^4}}, \quad (2.23)$$

which is the curve at which the local velocity of the string  $\mathbf{w} \rho(u)$  becomes equal to the local speed of light at this depth in the bulk as viewed from infinity, namely  $c_{\text{light}}(u) = \sqrt{1 - \frac{1}{u^4}}$ . However,  $\theta'$  itself must not change sign, since  $\theta'$  must be real. This can only be the case if the denominator of (2.21) changes sign at the same point that the numerator does, which implies that  $\rho_c^2(u_c^4 - 1) = \Pi^2$ . This condition uniquely specifies the point at which the solution describing a string worldsheet with a particular value of the constant  $\Pi$  must cross the curve  $\rho_{\text{light}}(u, \mathbf{w})$ , yielding

$$u_c = \sqrt{\frac{\Pi \mathbf{w}}{2} + \frac{1}{2} \sqrt{4 + \Pi^2 \mathbf{w}^2}}, \quad (2.24)$$

$$\mathbf{w} \rho_c = \sqrt{\frac{2 \Pi \mathbf{w}}{\Pi \mathbf{w} + \sqrt{4 + \Pi^2 \mathbf{w}^2}}}. \quad (2.25)$$

The rotating string solution starts at  $u = \infty$ ,  $\rho = \ell$ , passes through  $(u_c, \rho_c)$  and, we shall see, approaches the black hole horizon located at  $u = 1$  at a finite value of  $\rho$  that is greater than  $\rho_c$  which in turn is greater than  $\ell$ . The point  $(u_c, \rho_c)$  is completely analogous to one that occurs on the worldsheet of the string that trails behind and below a quark moving in a straight line at constant speed [11, 12]. As in that context, it demarcates the location of a horizon in the worldsheet metric  $g_{ab}$ . It separates the upper part of the string with  $u > u_c$  which moves slower than the local velocity of light from the lower part of the string with  $u < u_c$  whose local velocity exceeds that of light. By inspection of (2.17) and (2.23) we notice that  $\rho''$  appears in the equation of motion (2.18) multiplied by a factor which vanishes at  $(u_c, \rho_c)$ . This means that the equation of motion itself determines  $\rho'(u_c)$ , independent of any feature of the solution at any point away from  $(u_c, \rho_c)$ .<sup>2</sup> Therefore, small

---

<sup>2</sup>It is possible to show that  $\rho'(u_c)$  is given by the negative root of the equation

$$v_c \mathbf{w}^2 + \frac{4 \sqrt{1 - v_c^2} + \mathbf{w}^2}{(1 - v_c^2)^{\frac{1}{4}}} \rho'(u_c) - \frac{v_c^3}{1 - v_c^2} \rho'(u_c)^2 = 0 \quad (2.26)$$

where  $v_c \equiv \rho_c \mathbf{w}$ .



fluctuations of the string at  $u > u_c$  are causally disconnected from those at  $u < u_c$ , meaning in particular that the lower part of the string is disconnected from its endpoint on the D3-brane at the boundary [15, 13]. It has been argued recently that the lower part of such a string represents the “gluon cloud” that the quark has lost to the medium it is moving through (i.e. the energy it has “radiated”, using this phrase to encompass energy loss due to drag) while the upper part of the worldsheet represents the color fields carried within the quark wave function [19].

### 2.3 Radial dependence of the spiralling string

We have solved the radial equation of motion (2.18) for  $\rho(u)$ . In Fig. 1, we show results for  $\rho(u)$  for different combinations of the angular velocity  $\mathbf{w}$  and the constant of the motion  $\Pi$ . It proves convenient to use  $(u_c, \rho_c)$  as the initial point for the numerical evaluation. For each  $\Pi$ , the equations (2.24) and (2.25) tell us  $u_c$  and  $\rho_c = \rho(u_c)$ . And, as we saw in Section 2.2, the equations of motion then determine  $\rho'(u_c)$ . Knowing  $\rho(u_c)$  and  $\rho'(u_c)$ , we can solve the second order differential equation (2.18) for  $\rho(u)$  upward and downward from  $u_c$ , obtaining the solutions plotted in Fig. 1. Following the solution upwards to large  $u$  determines what value of  $\ell = \rho(\infty)$  corresponds to the value of  $\Pi$  whose selection specified the particular solution just constructed. From the perspective of the rotating quark at the boundary, the configuration is naturally specified by giving  $\ell$  and  $\mathbf{w}$ . From the perspective of the string to which this quark is attached, the configuration is naturally specified by  $\Pi$  and  $\mathbf{w}$ . Fig. 1 illustrates the fact that there is a one-to-one, and in fact monotonic, relationship between  $\ell$  and  $\Pi$ . Following the solution downwards, we find that at the horizon  $\rho(1)$  is finite; we shall see in the next subsection that there are nevertheless infinitely many coils of the spiral as the string approaches the horizon.

On the D3-brane at  $u = \infty$ , the rotating quark must not exceed the velocity of light. This limits the radius  $\ell$  to  $\ell < 1/\mathbf{w}$ . Indeed, we see in Fig. 1 that increasing  $\Pi$  without bound corresponds to increasing the  $u_c$  at which the velocity of the string exceeds the local velocity of light at that depth in the bulk, but it never causes  $\ell\mathbf{w}$  to exceed 1. Within the bulk, the string worldsheet bends towards larger values of  $\rho(u)$ , as the string approaches the horizon. This bending results from the centrifugal force which the rotating string experiences. It is more pronounced if the quark moves with greater acceleration  $\mathbf{a} = \mathbf{w}^2\ell$ . Indeed, we see from the figures that for a given  $\mathbf{w}$ , there is more bending for solutions with larger  $\ell$ . And, the increased bending with increasing  $\mathbf{w}$  is also manifest.

We see in Fig. 1 that for  $\mathbf{w} = 0.05$  and  $0.5$  the solutions  $\rho(u)$  change in character with increasing  $\Pi$ : for small enough  $\Pi$ ,  $\rho(1) \simeq \ell$  whereas for large enough  $\Pi$  the string bends outward sufficiently that  $\rho(1)$  becomes significantly larger than  $\ell$ . However, for  $\mathbf{w} = 5.0$  we find significant bending for any nonzero  $\Pi$ . We have checked these observations against more solutions than are shown in the figures themselves. We find that for  $\mathbf{w} > 1$  there seems to be no range of values of  $\Pi$  for which  $\rho(1) \simeq \ell$ . We will see in Section 3 that this crossover from string worldsheets that hang down at almost constant  $\rho$  to those that bend significantly outward is associated with a crossover in the parametric dependence of  $dE/dt$ , the energy that the rotating quark loses to the plasma that it is stirring. We have also investigated how  $\rho(1)$  changes with parameters in the regime in which it is  $\gg \ell$ . We find that  $\rho(1)$  tends to a finite limit if we increase  $\mathbf{w}$  while holding  $v$  fixed, while  $\rho(1)$  increases without bound if we take  $v \rightarrow 1$  while holding  $\mathbf{w}$  fixed.

For use in Section 3, we close this subsection by describing the behavior of  $\rho(u)$  in two limits:

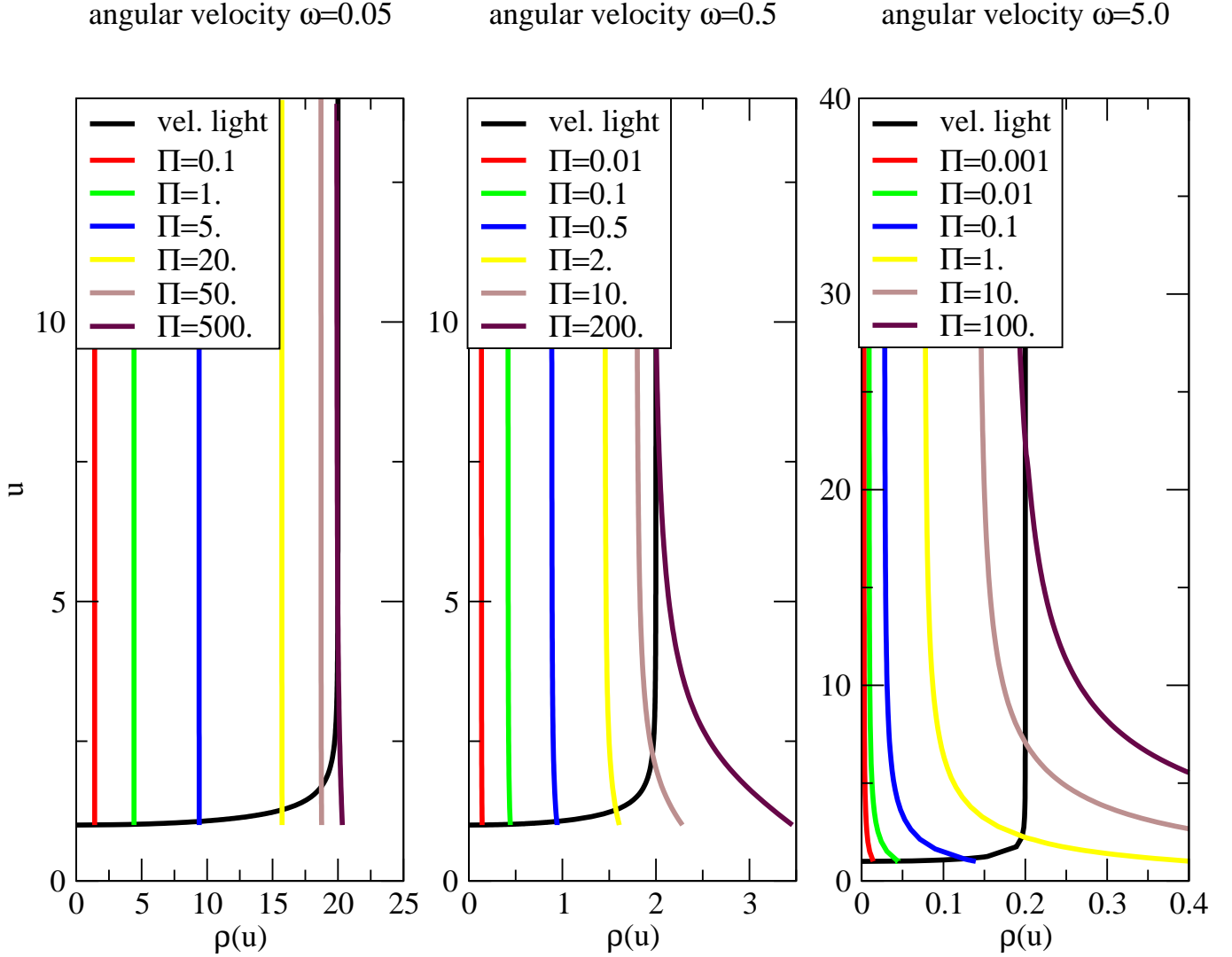


**Figure 1:** The radial dependence  $\rho(u)$  of string worldsheets describing the spiralling strings hanging down from rotating quarks with three choices of angular velocity,  $\omega = 0.05$ ,  $\omega = 0.5$  and  $\omega = 5.0$ , and a set of values for the constant of the motion  $\Pi$ . The figure shows that small (large) values of  $\Pi$  correspond to small (large) values of  $\rho(\infty) = \ell$ , the radius of the circle along which the quark at the boundary is moving. Each solution reaches the horizon  $u = 1$  at a finite  $\rho(1)$ . We also show the curve  $\rho_{\text{light}}(u, \omega)$ , given in (2.23), at which the string is moving at the local velocity of light. All the string solutions cross this curve, with those with smaller (larger) values of  $\Pi$  crossing it at smaller (larger) values of  $u$ .

1. The limit  $v = \ell\omega = \text{constant}$ ,  $\alpha = v\omega \rightarrow 0$ , meaning  $\omega \rightarrow 0$ .  
 In this limit, we can expand  $\rho(u)$  in (2.22) as a power series in  $\omega^2$ . Because we are taking  $\omega \rightarrow 0$  at fixed  $v$ , we must take  $\ell \propto 1/\omega \rightarrow \infty$ . The expansion of  $\rho$  therefore starts at order

$1/\mathfrak{w}$ , and so can be written as an expansion of  $v(u) \equiv \mathfrak{w}\rho(u)$ :

$$v(u) = v_0(u) + \mathfrak{w}^2 v_1(u) + \dots \quad (2.27)$$

To leading order, we then find from (2.22) that  $v'_0(u) = 0$ , meaning that  $v_0(u) = \text{constant} = \ell\mathfrak{w} = v$ . In this limit,  $\rho(u)$  is constant, meaning it is vertical in Fig. 1, and its value diverges proportional to  $1/\mathfrak{w}$ . We see from (2.25) that, because  $\rho(u)$  is constant and so  $\rho_c\mathfrak{w} = v$ , in this limit  $\Pi\omega \rightarrow \text{constant}$ .

2. The limit  $v = \ell\mathfrak{w} = \text{constant}$ ,  $\mathfrak{a} = v\mathfrak{w} \rightarrow \infty$ , meaning  $\mathfrak{w} \rightarrow \infty$ .

In this limit,  $\ell \propto 1/\mathfrak{w} \rightarrow 0$ . We find that in this limit  $\rho(1) \rightarrow \text{constant}$  even though  $\ell \rightarrow 0$  and, from (2.25),  $\rho_c \rightarrow 0$ , meaning that the ratio  $\rho(1)/\ell \rightarrow \infty$ . We shall discuss this limit further in Section 2.5, where we shall show that in this limit the string worldsheet takes on the same shape as in vacuum everywhere except near the horizon, and where we shall see that in this limit  $\Pi/\omega \rightarrow \text{constant}$ .

## 2.4 Angular dependence of the spiralling string

Having determined  $\rho(u)$  for a fixed angular velocity  $\mathfrak{w}$  and constant of motion  $\Pi$ , we can proceed to integrate  $\theta'$  given by (2.21). This equation determines  $\theta(u)$  up to an overall sign. The choice of this sign amounts to deciding whether the quark rotates clockwise or counter-clockwise in the  $(x_1, x_2)$ -plane. We choose the sign positive, which corresponds to clockwise rotation. In Fig. 2, we show a typical example of a complete solution for  $\rho(u)$  and  $\theta(u)$ , describing a spiralling string dragging behind and below a rotating quark. We see the string dropping down from the boundary and spiralling behind the rotating quark. The entire spiralling string in Fig. 2 is rotating with constant angular velocity. As  $u$  decreases,  $\rho(u)$  increases as we have already seen in Fig. 1. The angle

$$\theta(u) = \int_u^\infty \theta'(\tilde{u}) d\tilde{u} \quad (2.28)$$

increases. (Recall that  $\theta'$  is given by (2.21).) For  $u \rightarrow 1$ , the curve approaches the horizon at a finite radius  $\rho(1)$ , with  $\rho'(1)$  also finite. In approaching  $u \rightarrow 1$ , the string coils around the center of motion of the quark infinitely many times. This can be seen from (2.21) by noting that as  $u \rightarrow 1$ ,  $\theta'$  has a singularity  $\propto 1/(u-1)$ . Consequently, there is a logarithmic increase in  $\theta(u)$  as  $u \rightarrow 1$ . Explicitly, if we define  $\Delta\theta(u)$  as the angle swept out by the string as it descends from some reference value of  $u$ , which we denote  $u_0$ , that is already close to the horizon,  $u_0 - 1 \ll 1$ , down to values of  $u$  that are even closer to the horizon, then

$$\Delta\theta(u) = \int_u^{u_0} \theta'(\tilde{u}) d\tilde{u} \simeq \int_u^{u_0} \frac{\mathfrak{w}}{\tilde{u}^4 - 1} d\tilde{u} \simeq \int_u^{u_0} \frac{\mathfrak{w}}{4(\tilde{u} - 1)} = \frac{\mathfrak{w}}{4} \ln \left[ \frac{u_0 - 1}{u - 1} \right]. \quad (2.29)$$

This behavior of  $\theta(u)$  near the horizon is quite analogous to the behavior of the trailing string hanging from a quark moving with constant linear velocity,  $x_1 = vt$ . This string worldsheet is given by [11, 12]

$$x_1(u, t) = vt - \frac{v}{2} \left[ \frac{\pi}{2} - \arctan u - \text{arccoth } u \right], \quad (2.30)$$

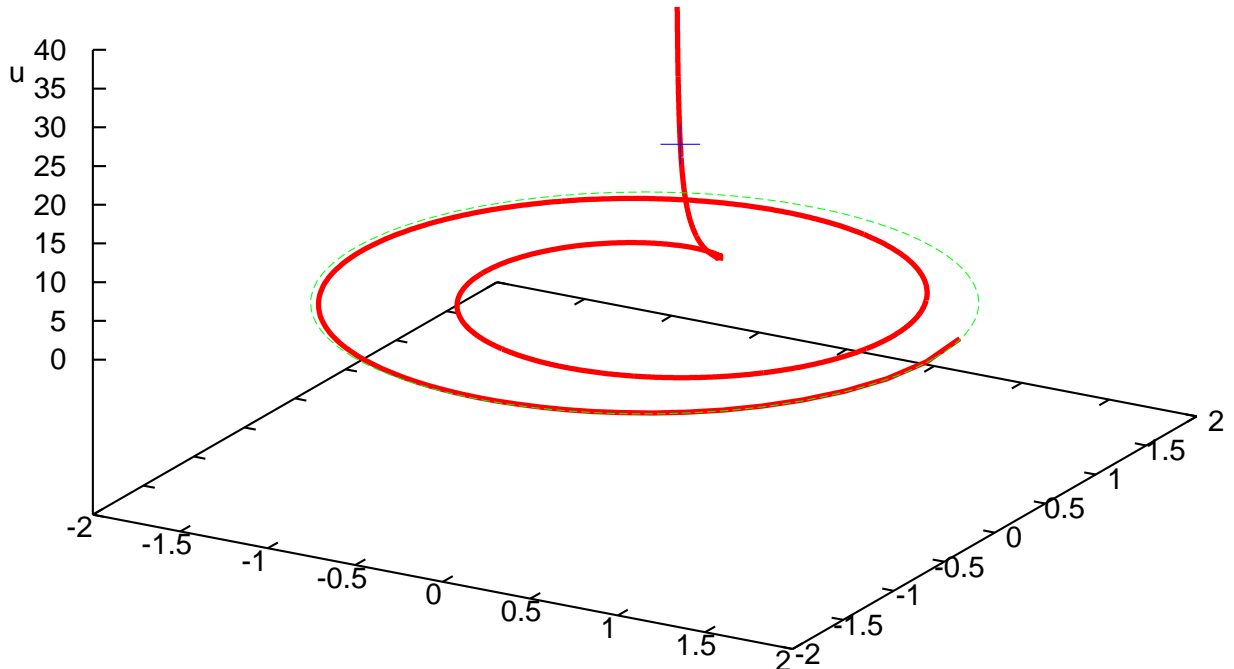


**Figure 2:** The rotating string solution for  $\omega = 5.$  and  $\Pi = 100.$ . The quark rotates clockwise at the boundary at a radius  $\ell = \rho(\infty) = 0.1789.$  This corresponds to a relativistic quark moving with speed  $v = 0.895.$  The cross marks the depth at which the velocity of the string exceeds the local velocity of light. We have ended the plot at  $u = 1.005,$  but the solution actually spirals downward forever, with infinitely many coils getting ever closer to the horizon at  $u = 1.$  The radii of these coils tend to  $\rho(1) = 1.65004,$  significantly greater than  $\ell$  but finite. The dashed (green) circle denotes  $\rho = \rho(1)$  at  $u = 1.$

with both  $t$  and  $x_1$  measured in units of  $1/(\pi T).$  This means that

$$x'_1 = \frac{v}{u^4 - 1} \simeq \frac{v}{4(u - 1)} \quad (2.31)$$

in the vicinity of the horizon. The logarithmic divergence of the length of this trailing straight string and of the length of our trailing rotating string are clearly analogous. They are not the

same because the quantity  $\rho(1)\mathbf{w}$  which appears in (2.29) in the same way that the linear velocity  $v$  appears in (2.31) is in fact greater, and in some instances much greater, than the speed of the rotating quark, which is given by  $\ell\mathbf{w}$ .

## 2.5 Rotating quark in vacuum

In the next Section, we shall want to compare the energy lost by a rotating quark in the hot plasma of strongly coupled  $\mathcal{N} = 4$  SYM theory to that lost by a rotating quark in vacuum in the same theory. To that end, it will be useful to understand the ways in which the trailing string in vacuum is similar to or different from the trailing string in the plasma that we have constructed. In vacuum, the string describes the energy radiated from the rotating quark due to its acceleration. The calculation in vacuum proceeds analogously to that above, and we therefore need only sketch it briefly.

In vacuum, the Lagrangian (2.17) and the equations of motion (2.21) and (2.22) simplify to

$$\mathcal{L} = \sqrt{(1 - \rho^2\mathbf{w}^2)(u^4\rho'^2 + 1) + \rho^2u^4\theta'^2} \quad (2.32)$$

and

$$\theta'^2 = \frac{\Pi^2 (1 - \rho^2\mathbf{w}^2)(u^4\rho'^2 + 1)}{\rho^2u^4(\rho^2u^4 - \Pi^2)}, \quad (2.33)$$

and

$$\rho'' + \frac{2\rho'}{u} + (1 + \rho'^2u^4)\rho \left( \frac{2u^3\rho\rho' - 1}{u^4\rho^2 - \Pi^2} + \frac{1}{\rho^2u^4(1 - \rho^2\mathbf{w}^2)} \right) = 0, \quad (2.34)$$

where  $\Pi = \partial\mathcal{L}/\partial\theta'$  is a constant of the motion as before and where the dimensionless variables  $u$ ,  $\rho$ , and  $\mathbf{w}$  are now related to their dimensionful counterparts by  $u = \tilde{u}/R$ ,  $\rho = \tilde{\rho}/R$ , and  $\mathbf{w} = \omega R$  instead of (2.11), (2.12) and (2.14).

As before, the denominator of (2.33) vanishes at some  $u_c$  and becomes negative for  $u < u_c$ , meaning that the numerator of (2.33) must vanish at the same  $u_c$ . In vacuum, this worldsheet horizon where the string velocity equals the local speed of light is located at

$$u_c^{\text{vac}} = \sqrt{\Pi\mathbf{w}}, \quad (2.35)$$

$$\rho_c^{\text{vac}} = \frac{1}{\mathbf{w}}. \quad (2.36)$$

As before, choosing  $\Pi$  determines  $(u_c^{\text{vac}}, \rho_c^{\text{vac}})$  and the equation of motion (2.34) can then be solved starting from this point. Following the solution upwards determines  $\ell$ , where  $\ell R$  is the radius of the circle at  $u = \infty$  along which the quark is moving. Notice that in the large  $\Pi\mathbf{w}$  limit, the location of the world sheet horizon for a quark rotating in plasma given by (2.24) and (2.25) tends to  $(u_c^{\text{vac}}, \rho_c^{\text{vac}})$ . Correspondingly, we find that if we choose  $\Pi\mathbf{w}$  to be large, the solution  $\rho(u)$  that we obtain by solving (2.34) for  $u > u_c^{\text{vac}}$  is very similar to that which we found previously in plasma for  $u > u_c$ .

Following the solution  $\rho(u)$  downwards from  $(u_c^{\text{vac}}, \rho_c^{\text{vac}})$ , we find that in this regime the string worldsheet is qualitatively different in vacuum relative to that which we found previously in the plasma. Recall that in the plasma the solution extends down toward the horizon at  $u = 1$ , where

$\rho(1)$  is finite and where  $\theta(u)$  increases logarithmically as  $u \rightarrow 1$ . Instead, in vacuum the solution extends down toward  $u = 0$  and it is easy to show from (2.34) and (2.33) that as  $u \rightarrow 0$  the solution takes the form

$$\rho(u) \approx \frac{f}{u} + \dots \quad (2.37)$$

$$\theta(u) \approx \frac{\sqrt{1+f^2}}{u} + \dots \quad (2.38)$$

for some constant  $f$ , meaning that the spiralling string world sheet extends to  $\rho \rightarrow \infty$  as  $u \rightarrow 0$ . We shall discuss the interpretation of this qualitative distinction between the pattern of energy deposited by a quark rotating in vacuum and one rotating in the plasma in Section 3.2.

It is instructive to notice that if we rescale  $u$  and  $\rho$  by introducing new variables  $u/\mathbf{w}$  and  $\mathbf{w}\rho$  then, when written in terms of the new variables, both the equations of motion (2.33) and (2.34) include  $\Pi$  and  $\mathbf{w}$  only in the combination  $\Pi/\mathbf{w}$ . This means that there is a one-to-one map between the velocity of the quark  $v$  and the ratio  $\Pi/\mathbf{w}$ . Even though this simplification of the vacuum equations does not occur in the  $T \neq 0$  equations, it prompts us to return to the equation of motion (2.22) for  $\rho(u)$  at  $T \neq 0$  and reconsider the limit in which we take  $\mathbf{w} \rightarrow \infty$  at fixed  $v$ , introduced briefly in Section 2.3. If we rewrite (2.22) in terms of  $u/\mathbf{w}$  and  $\mathbf{w}\rho$  it still contains both  $\Pi/\mathbf{w}$  and  $\mathbf{w}$ , but if we then take the  $\mathbf{w} \rightarrow \infty$  limit at fixed  $\Pi/\mathbf{w}$  by expanding the equation to zeroth order in powers of  $1/\mathbf{w}$  we find that we recover the zero temperature equation (2.34), with (2.24) and (2.25) becoming (2.35) and (2.36) as we already saw. Thus, in this scaling limit the nonzero temperature and zero temperature solutions  $\rho(u)$  become identical for  $u \geq u_c$  and the relation between  $\Pi/\mathbf{w}$  and the quark velocity  $v$  becomes the same as in vacuum. However, this analysis breaks down near the black hole horizon. At the horizon,  $\rho(u) \rightarrow \rho(1) = \text{constant}$  in the  $\mathbf{w} \rightarrow \infty$  at fixed  $v$  limit, meaning that  $\mathbf{w}\rho(1) \propto \mathbf{w}$ . This rearranges the  $1/\mathbf{w}$ -expansion of (2.22) in the vicinity of the horizon, since what must now be expanded is the equation written in terms of  $\rho$  rather than  $\mathbf{w}\rho$ . The  $T \neq 0$  equation of motion then no longer reduces to its vacuum form. Our numerical solutions confirm that for all  $u > u_c$  and for much of the  $u < u_c$  region (but not near  $u = 1$ ) as we increase  $\mathbf{w}$  at fixed  $\Pi/\mathbf{w}$ , and hence at fixed  $v$ , the solution  $\rho(u) \propto 1/\mathbf{w} \rightarrow 0$  and approaches its shape in vacuum. Near the horizon, however, where (2.22) does not become (2.34), we have  $\rho(u) \rightarrow \rho(1) = \text{constant}$ . This difference between the behavior of  $\rho(u)$  near the horizon and its behavior in vacuum is responsible for the difference between (2.37) and (2.38) and the behavior of  $\rho$  and  $\theta$  near the horizon at  $T \neq 0$ , described in Sections 2.3 and 2.4.

### 3. Energy Lost by a Rotating Quark

#### 3.1 General and numerical results

As Herzog *et al* and Gubser showed for the case of a quark moving in a straight line with constant speed [11, 12], in a setting in which a moving quark in the boundary theory is described by a string worldsheet whose shape does not change with time, the energy lost by the moving quark is easy to evaluate once the shape of the string worldsheet has been determined. The energy deposited in

the medium per unit time (or, equivalently, the power expended by the external agent moving the quark) is given by

$$\frac{dE}{dt} = \Pi_t^\sigma, \quad (3.1)$$

where

$$\Pi_\mu^\sigma \equiv \frac{1}{2\pi\alpha'} \frac{\partial \mathcal{L}}{\partial (\partial_\sigma X^\mu)} = -G_{\mu\nu} \frac{[(\partial_u X) \cdot (\partial_\tau X)] \partial_\tau X^\nu - [(\partial_\tau X) \cdot (\partial_\tau X)] \partial_u X^\nu}{2\pi\alpha' \sqrt{-\det g_{ab}}} \quad (3.2)$$

gives the flow of either energy ( $\mu = t$ ) or momentum down the string. For the rotating string that we have analyzed in Sections 2.1-2.4, explicit evaluation yields a result with the simple form

$$\frac{dE}{dt} = \frac{\pi}{2} \sqrt{\lambda} T^2 \mathbf{w} \Pi, \quad (3.3)$$

where we have restored all the dimensionful factors and have used (2.3).<sup>3</sup>

It will prove instructive to recast our result (3.3) for the energy loss in terms of the location  $(u_c, \rho_c)$  of the point at which the velocity of the rotating string exceeds the local velocity of light at that depth in the bulk or, equivalently, the location of the worldsheet horizon. By solving (2.25) for  $\Pi \mathbf{w}$ , we find that  $dE/dt$  in (3.3) is given by

$$\frac{dE}{dt} = \frac{\pi}{2} \sqrt{\lambda} T^2 \frac{v_c^2}{\sqrt{1 - v_c^2}}, \quad (3.5)$$

where  $v_c \equiv \mathbf{w} \rho_c$  is the velocity of the string at the point where that velocity is also the local velocity of light. We can compare our result (3.5) to  $dE/dt$  for a quark moving in a straight line with speed  $v$ , which is easily obtained from the string worldsheet (2.30) and is given by [11, 12]

$$\left. \frac{dE}{dt} \right|_{\text{linear drag}} = \frac{\pi}{2} \sqrt{\lambda} T^2 \frac{v^2}{\sqrt{1 - v^2}}. \quad (3.6)$$

Because the general result (3.3) for the energy loss of a rotating quark takes the form (3.5), it is identical to that for a quark in linear motion with velocity  $v_c$ . Wherever  $v_c \simeq v$ , the standard linear drag result for  $dE/dt$  is obtained. Wherever the outward curvature of the string worldsheet

---

<sup>3</sup>We have checked that the same result can also be obtained by evaluating

$$\frac{dE}{dt} = -\frac{d}{dt} \int du \Pi_t^\tau \quad (3.4)$$

(where  $\Pi_t^\tau$ , which can be obtained by interchanging  $\tau$  and  $\sigma$  in (3.2), is the energy density  $dE/du$  along the string) upon choosing any time independent upper cutoff to the  $u$ -integral and upon choosing a (time-dependent) lower cutoff to the  $u$ -integral corresponding to the  $u$  of the string worldsheet at some fixed angle  $\theta$ .

in Fig. 1 is significant, making  $v_c$  significantly greater than  $v$ ,  $dE/dt$  is greater. We shall interpret this result further in Section 3.2.<sup>4</sup>

The result (3.3) makes it straightforward to use the numerical calculations described in Section 2 to evaluate the energy loss  $dE/dt$  for a quark moving in a circle with angular frequency  $\omega = \mathbf{w}\pi T$  as a function of the radius of the circle  $L = \ell/(\pi T)$ , as follows. We pick  $\mathbf{w}$  and we pick a series of values of  $\Pi$ . For each  $\Pi$ , we follow the procedure described in Section 2 to obtain the corresponding string worldsheet. From that solution, we determine  $\ell$  at large  $u$ . Then, since  $dE/dt$  is just a constant times  $\Pi$ , we plot  $\Pi$  as a function of  $\ell$ , obtaining the plots in the first row of Fig. 3. We see that  $\Pi$ , and hence  $dE/dt$ , increase without bound as  $\ell$  approaches  $1/\mathbf{w}$ , which is the radius at which the quark would be moving at the speed of light.

### 3.2 Energy loss in two limits: linear drag and vacuum radiation

Numerical results for  $dE/dt$ , as in the first row of Fig. 3, are not very informative until they are compared to analytic expectations or explanations. There are two limits to consider:

1. The limit  $v = \ell\mathbf{w} = \text{constant}$ ,  $\mathfrak{a} = v\mathbf{w} \rightarrow 0$ .

This limit is reached by increasing  $\ell$  and decreasing  $\mathbf{w}$  while keeping  $v$  fixed. Because we are taking the (dimensionless) acceleration to zero, in this limit we expect  $dE/dt$  to be given by the result (3.6) for a quark moving in a straight line with speed  $v$ , meaning that we expect that as  $\mathfrak{a} \rightarrow 0$  at fixed  $v$  we should find that  $dE/dt$  for the rotating quark is given by (3.3) with

$$\mathbf{w}\Pi \rightarrow \mathbf{w}\Pi_{\text{linear drag}} \equiv \frac{v^2}{\sqrt{1-v^2}}, \quad (3.9)$$

meaning that holding  $v$  fixed as we take the  $\mathbf{w} \rightarrow 0$  limit means holding  $\Pi\mathbf{w}$  fixed. The general result (3.5) for  $dE/dt$  together with the result from Section 2.3 that  $\rho(u) = \ell = \text{constant}$  and therefore  $v_c = v$  in the present limit constitute an analytic demonstration of (3.9). In the second row of Fig. 3, we show the ratio of our numerically obtained results for  $\Pi$  for the rotating quark to  $\Pi_{\text{linear drag}}$ . We see that our  $dE/dt$  is described well by that for a quark in linear motion when  $\ell$  is small enough at  $\mathbf{w} = 0.05$  and  $\mathbf{w} = 0.5$ , i.e. in the regime where  $\mathfrak{a}$  is small. Surprisingly, we see in the panel with  $\mathbf{w} = 5.0$  that once the dimensionless frequency is large enough,  $\Pi \gg \Pi_{\text{linear drag}}$  even at small  $\ell$ , where the dimensionless acceleration  $\mathfrak{a} = \ell\mathbf{w}^2$  is small. So, the criterion for the validity of the linear drag approximation to our result for the energy loss of a rotating quark cannot be simply  $\mathfrak{a} \rightarrow 0$ .

---

<sup>4</sup>In order to make contact with Ref. [19], we can instead solve (2.24) for  $\Pi\mathbf{w}$ , finding that  $dE/dt$  in (3.3) is given by

$$\frac{dE}{dt} = \frac{\pi}{2} \sqrt{\lambda} T^2 \frac{u_c^4 - 1}{u_c^2}. \quad (3.7)$$

In the  $v = \ell\mathbf{w} \rightarrow 1$  limit, where the worldsheet horizon  $u_c \rightarrow \infty$ , we see from (2.24) that  $u_c \simeq \sqrt{\mathbf{w}\Pi}$ , yielding the even simpler result

$$\frac{dE}{dt} = \frac{\pi}{2} \sqrt{\lambda} T^2 u_c^2. \quad (3.8)$$

At high velocity we therefore reproduce the relationship between  $dE/dt$  and the worldsheet horizon for a quark moving in a straight line at constant velocity in the high velocity limit that has been emphasized in Ref. [19].



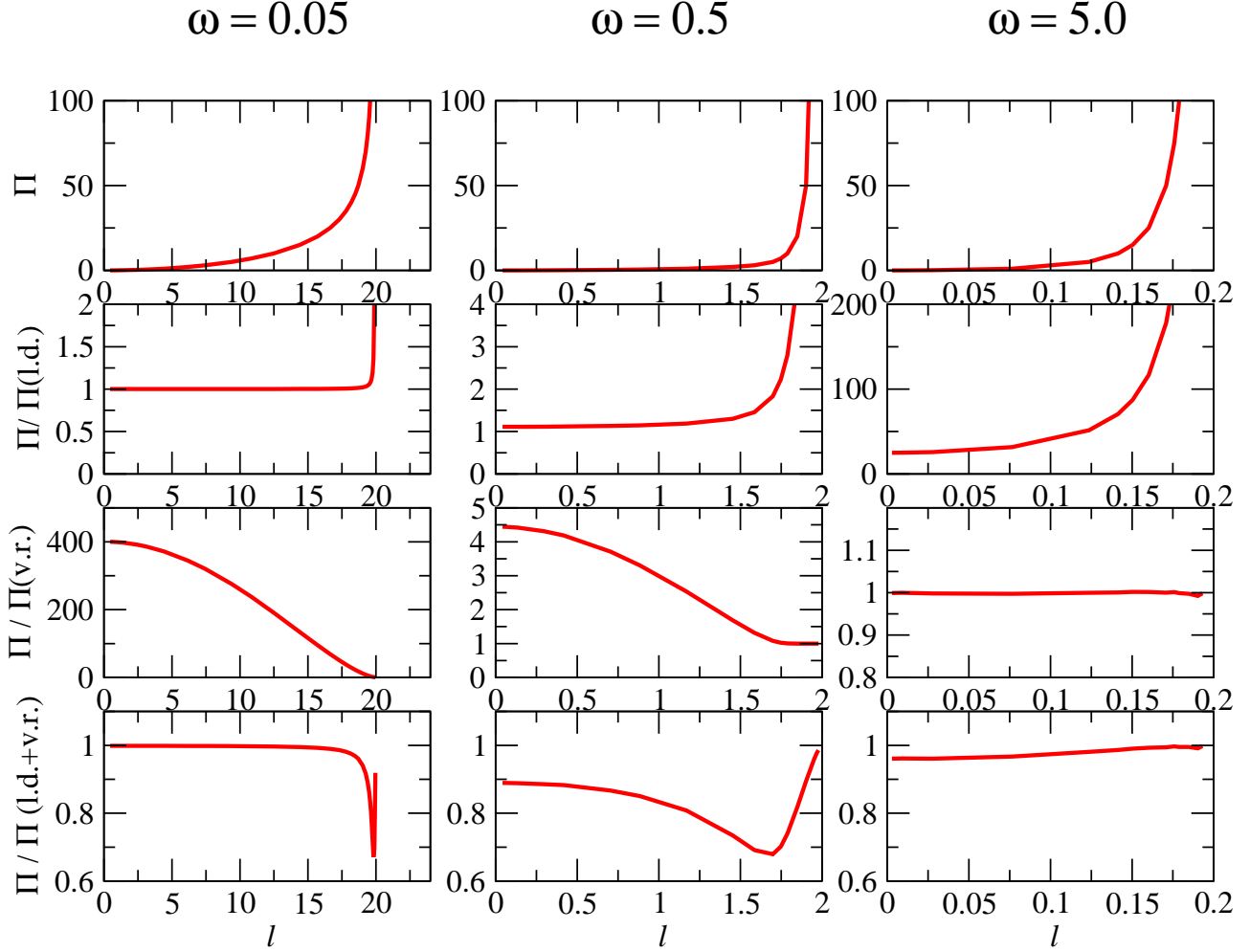


**Figure 3:** Upper row:  $\Pi$ , which is proportional to the rate of energy loss  $dE/dt$  according to (3.3), plotted as a function of the dimensionless radius  $\ell$  at which the quark rotates, for three different values of the dimensionless angular velocity  $\omega$ . Second row:  $\Pi/\Pi_{\text{linear drag}}$ , where  $\Pi_{\text{linear drag}}$  is given in (3.9) and is what we expect to find if  $dE/dt$  is given by that due to the drag on a quark moving in a straight line with velocity  $v = \ell\omega$ . We see that at  $\omega = 0.05$  and  $0.5$ ,  $\Pi \simeq \Pi_{\text{linear drag}}$  at low enough  $\ell$ , i.e. at low enough acceleration  $\alpha$ . At  $\omega = 5.0$ , however,  $\Pi$  exceeds  $\Pi_{\text{linear drag}}$  by a large factor at any  $\ell$ , e.g. by a factor of 24.980 for  $\ell \rightarrow 0$  and hence  $\alpha \rightarrow 0$ . Third row:  $\Pi/\Pi_{\text{vacuum radiation}}$ , where  $\Pi_{\text{vacuum radiation}}$  is given in (3.13) and is what we would find if  $dE/dt$  is given by the energy loss due to the radiation of an accelerating charged particle in vacuum. We see that  $\Pi \simeq \Pi_{\text{vacuum radiation}}$  at large enough  $\ell$  for  $\omega = 0.05$  and  $0.5$  and at all  $\ell$  (and hence all  $v$  and  $\alpha$ ) for  $\omega = 5.0$ . Bottom row: The ratio  $\Pi/(\Pi_{\text{vacuum radiation}} + \Pi_{\text{linear drag}})$  is smaller than one for all  $\omega$  and all  $\ell$ , supporting the picture that there is destructive interference between acceleration-induced radiation and medium-induced radiation.

Given the general result (3.5), the validity of the linear drag approximation can be related directly to the shape of the string profile  $\rho(u)$ , as in Fig. 1. Whenever  $\rho(u)$  is to a good approximation constant, meaning that the curves in Fig. 1 are to a good approximation

vertical,  $\rho_c \simeq \ell$  and hence  $v_c \simeq v$ , meaning that in this circumstance the general result (3.5) becomes (3.9), as for a quark in linear motion.

2. The limit  $v = \ell \mathbf{w} = \text{constant}$ ,  $\mathfrak{a} = v \mathbf{w} \rightarrow \infty$ .

This limit is reached by decreasing  $\ell$  and increasing  $\mathbf{w}$  while keeping  $v$  fixed. In this limit, we expect the effects of acceleration to dominate. And, we have seen in Sections 2.3 and 2.5 that in this limit the shape of the spiralling string at  $u > u_c$  — above the worldsheet horizon — is the same at  $T \neq 0$  as it is in vacuum. This means that we expect that  $dE/dt$  for the quark stirring the strongly coupled plasma in this acceleration-dominated regime should be the same as if the quark were rotating in vacuum. And, in Ref. [20] Mikhailov has derived an elegant and general result for  $dE/dt$  for an accelerating quark in  $\mathcal{N} = 4$  SYM theory at  $T = 0$ , i.e. in vacuum, where  $dE/dt$  is due to (synchrotron) radiation. Mikhailov's result is

$$\left. \frac{dE}{dt} \right|_{\text{vacuum radiation}} = \frac{\sqrt{\lambda}}{2\pi} \frac{\vec{a}^2 - (\vec{a} \times \vec{v})^2}{(1 - v^2)^3}. \quad (3.10)$$

This result is equivalent to Liénard's result for electromagnetic radiation from an accelerating charge [21] upon replacing  $2e^2/3$  in the latter by  $\sqrt{\lambda}/(2\pi)$ . For the case of circular motion, Mikhailov's result becomes

$$\left. \frac{dE}{dt} \right|_{\text{vacuum radiation}} = \frac{\sqrt{\lambda}}{2\pi} \frac{a^2}{(1 - v^2)^2} \equiv \frac{\sqrt{\lambda}}{2\pi} a_{\text{proper}}^2, \quad (3.11)$$

where we have defined the proper acceleration in the usual fashion. So, if in the  $\mathfrak{a} \rightarrow \infty$  at fixed  $v$  limit  $dE/dt$  for our rotating quark is as it would be due to radiation in vacuum, we should find that  $dE/dt$  is given by (3.3) with

$$\pi^2 T^2 \mathbf{w} \Pi \rightarrow a_{\text{proper}}^2, \quad (3.12)$$

namely

$$\mathbf{w} \Pi \rightarrow \mathbf{w} \Pi_{\text{vacuum radiation}} \equiv \mathfrak{a}_{\text{proper}}^2 \equiv \frac{\mathfrak{a}^2}{(1 - v^2)^2} = \frac{v^2 \mathbf{w}^2}{(1 - v^2)^2}, \quad (3.13)$$

meaning that holding  $v$  fixed as we take the  $\mathbf{w} \rightarrow \infty$  limit means holding  $\Pi/\mathbf{w}$  fixed. In the third row of Fig. 3, we show the ratio of our numerically obtained results for  $\Pi$  for the rotating quark to  $\Pi_{\text{vacuum radiation}}$ . We see that our  $dE/dt$  is described well by that for a quark in circular motion that is radiating in vacuum when  $\ell$  is close enough to  $1/\mathbf{w}$  at any  $\mathbf{w}$ . Thus, in the large  $\mathfrak{a}$  limit the energy loss of a quark that is stirring the plasma is the same as it would be due to its acceleration if it were rotating in vacuum. Furthermore, the  $\mathbf{w} = 5.0$  panel shows that at large enough  $\mathbf{w}$  this result extends to all  $\ell$ , including down to values of  $\ell$  that are small enough that  $\mathfrak{a}$  is small. So, the criterion for the validity of the vacuum radiation approximation to our result for the energy loss of the rotating quark cannot be simply  $\mathfrak{a} \rightarrow \infty$ .

It turns out that the correct criterion for determining under what circumstances  $dE/dt$  is as it would be due to the drag on a quark moving in a straight line with the same  $v$  and under what

circumstances it is as it would be due to radiation if the quark were rotating in vacuum is given simply by asking which of the two yields the larger  $dE/dt$ .  $dE/dt|_{\text{vacuum radiation}} \gg dE/dt|_{\text{linear drag}}$  when  $\Pi_{\text{vacuum radiation}} \gg \Pi_{\text{linear drag}}$ , namely when

$$\mathbf{w} \gg (1 - v^2)^{3/4}, \quad (3.14)$$

where we have used (3.9) and (3.13). We see in particular that energy loss due to radiation in vacuum is larger than that due to linear drag in a plasma when  $\mathbf{w} > 1$  for any  $v$ . This explains the right panels of Fig. 3. In the middle and left panels of Fig. 3, the location of the crossover between  $dE/dt \simeq dE/dt|_{\text{linear drag}}$  at lower  $\ell$  and  $dE/dt \simeq dE/dt|_{\text{vacuum radiation}}$  at higher  $\ell$  is well described by the criterion (3.14). Furthermore, we find that the regime where the  $\gg$  in (3.14) is a  $\sim$  is the same regime where, in Section 2, we saw the radial profile  $\rho(u)$  of the spiralling string hanging down from the rotating quark begin to bend outward significantly. Where the  $\gg$  in (3.14) is a  $\ll$ , the  $\rho(u)$  curves in Fig. 1 are vertical to a very good approximation.

If we plot  $\Pi/(\Pi_{\text{linear drag}} + \Pi_{\text{vacuum radiation}})$  as in the fourth row of Fig. 3, we find that  $\Pi \simeq (\Pi_{\text{linear drag}} + \Pi_{\text{vacuum radiation}})$  in the regimes where one or other dominates, and in the crossover between the drag-dominated regime and the acceleration-radiation-dominated regime we find  $\Pi < (\Pi_{\text{linear drag}} + \Pi_{\text{vacuum radiation}})$ , as if the two sources of energy loss were interfering destructively. For sufficiently small  $\omega$ , the minimum in the ratio  $\Pi/(\Pi_{\text{linear drag}} + \Pi_{\text{vacuum radiation}})$  is at about  $2/3$ , and this minimum occurs close to the point at which the inequality (3.14) turns into an equality, namely  $\ell = \sqrt{1 - \omega^{4/3}}/\omega$ .

The interplay between energy loss due to linear drag and energy loss due to acceleration-induced radiation as if in vacuum can be illustrated in a single figure by plotting  $\Pi\mathbf{w}/(\gamma v^2)$  versus  $\mathbf{w}^2\gamma^3$ , where  $\gamma \equiv 1/\sqrt{1 - v^2}$ . The resulting Fig. 4 illustrates clearly that the energy loss is dominated by linear drag when  $\mathbf{w}^2\gamma^3 \ll 1$  and by radiation as if in vacuum when  $\mathbf{w}^2\gamma^3 \gg 1$ , as in (3.14). We understand from (3.9) and (3.13) why the curves with different values of  $\mathbf{w}$  lie on top of each other in these regimes, but we have no analytical argument why there should be a single scaling curve in the crossover regime. We observe, however, that the curves come very close to lying on a single universal scaling curve even in the crossover regime. Looking back at Fig. 3, we realize from Fig. 4 that the dips in the curves in the lower left and lower middle plots in Fig. 3 would have the same shape if they were plotted versus  $\mathbf{w}^2\gamma^3$ , rather than versus  $\ell$ . In Fig. 4 we have also illustrated the evidence for destructive interference between energy loss due to radiation as if in vacuum and energy loss due to drag by showing that our results lie below where they would have been if the energy loss were simply the incoherent sum of that due to these two mechanisms.

Our results illustrate that the analysis of the energy loss of a rotating quark that is stirring the plasma allows us to study the crossover from a linear-drag-dominated regime to an acceleration-dominated regime in a calculation that is valid in both regimes. (In Section 3.3, we shall discuss where our calculation breaks down.) In the acceleration-dominated regime,  $dE/dt$  is as it would be in vacuum. We can give a partial explanation for this phenomenon. Given that Mikhailov's result for radiation of an accelerating charge in  $\mathcal{N} = 4$  SYM differs only by the coupling constant from Liénard's result for QED, it is natural to expect that, as in QED, the spectrum of the synchrotron radiation rises gradually with increasing frequency until frequencies  $\simeq \omega_c$ , and then falls

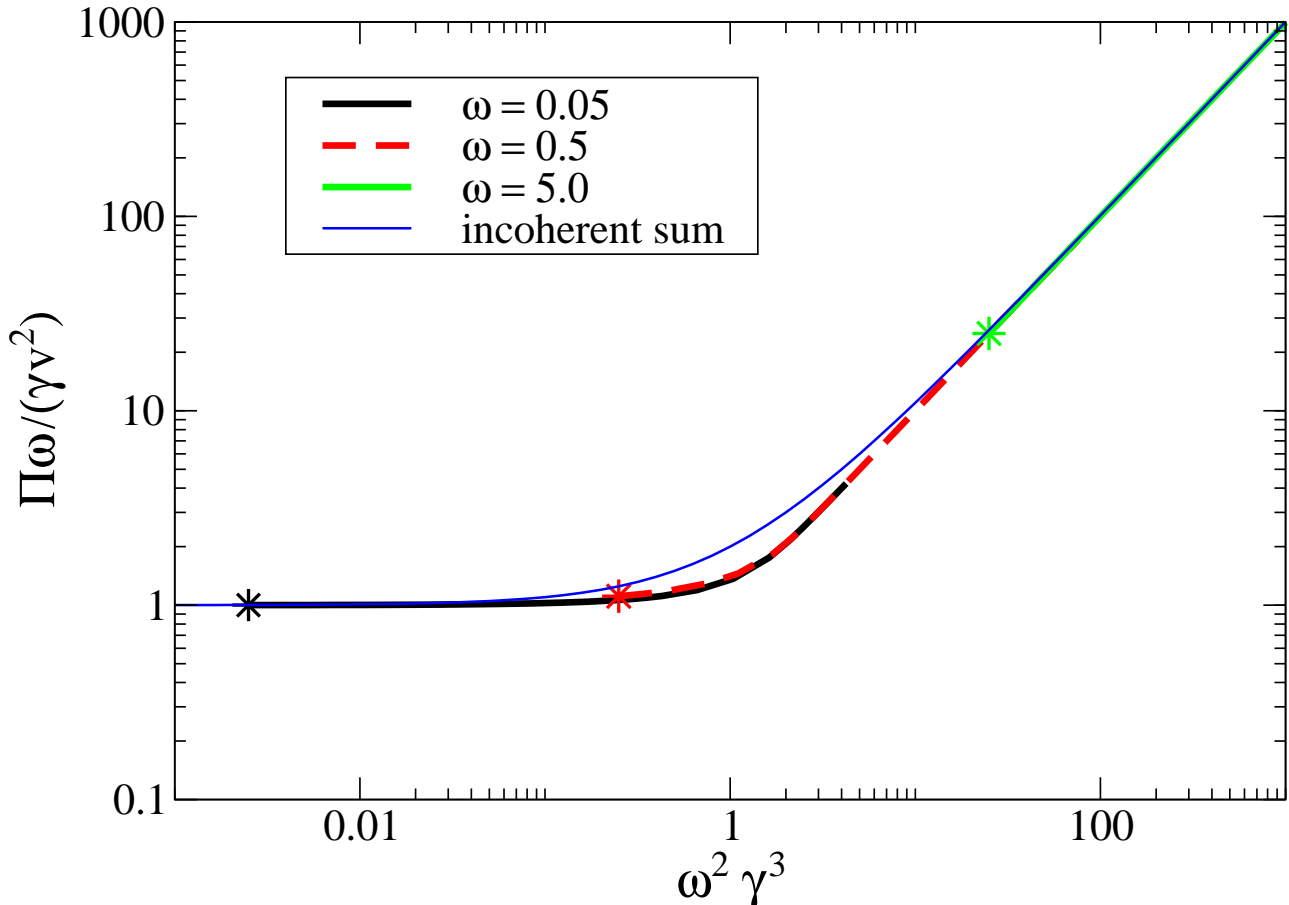


**Figure 4:** Scaled energy loss versus scaled velocity. By plotting  $\Pi\omega/(\gamma v^2)$  versus  $\omega^2\gamma^3$ , we can illustrate the crossover between the regime in which energy loss is dominated by drag — where  $\Pi\omega/(\gamma v^2) = 1$  — and the regime in which energy loss is dominated by radiation as if in vacuum — where  $\Pi\omega/(\gamma v^2) = \omega^2\gamma^3$ . Furthermore, using these scaled variables our results for any value of  $\omega$  come close to falling on a single curve. For each of the three values of  $\omega$  plotted, the star marks the point at which  $v = 0$  and  $\gamma = 1$  and the curve extends from the star arbitrarily far to the right as  $\gamma$  increases. For any  $\omega$ , the regime where radiation due to acceleration dominates the energy loss is reached at large enough  $\gamma$ ; for  $\omega = 5$ , the energy loss is in this regime already at  $\gamma = 1$ . We have also plotted  $\Pi\omega/(\gamma v^2) = 1 + \omega^2\gamma^3$ , which is the result that we would have obtained if the energy loss were the incoherent sum of that due to drag and that due to radiation as if in vacuum. Our results lie below this curve, indicating destructive interference.

off exponentially for frequencies that are  $\gg \omega_c$ , with the critical frequency being given by

$$\omega_c = 3\gamma^3\omega, \quad (3.15)$$

with  $\gamma = 1/\sqrt{1-v^2}$  and  $\omega$  the dimensionful angular frequency of the rotating charge. This means that almost all of the radiated energy is carried by radiation modes with frequencies of order  $\omega_c$ . And, in any circumstance in which the criterion (3.14) is satisfied,  $\omega_c \gg \pi T$ . (To see this, note that (3.14) can either be satisfied via  $\omega \gg 1$ , which means  $\omega \gg \pi T$  and hence  $\omega_c \gg \pi T$  even if  $\gamma$

is not large, or (3.14) can be satisfied at small  $\mathbf{w}$  for values of  $\gamma$  that are large enough that, again,  $\omega_c \gg \pi T$ .) So, if the plasma were weakly coupled we could conclude that radiation into modes with frequencies  $\omega_c \gg \pi T$  is unaffected by the presence of the plasma and thus understand why  $dE/dt$  in the acceleration-dominated regime (3.14) is as it would be if the rotating quark were emitting synchrotron radiation in vacuum. However, in  $\mathcal{N} = 4$  SYM we have a plasma that is strongly coupled at all scales. And, the synchrotron radiation is composed of colored excitations rather than neutral photons. We do not expect that any excitations propagate for times large compared to the inverse of the temperature — there are after all no long-lived quasiparticles expected in this system. And, we expect any energetic colored excitations to be strongly quenched by the plasma.

The shape of the spiralling string worldsheet trailing behind the rotating quark, as in Fig. 2 provides direct evidence that the behavior of the energy that is deposited in the plasma by the rotating quark is different from that of synchrotron radiation in vacuum even in the acceleration-dominated regime in which  $dE/dt$  is as for vacuum radiation. We saw in Section 2.5 that when we redo our calculation in vacuum, the rotating string extends out to  $\rho \rightarrow \infty$ . This corresponds to the fact that, in vacuum, the energy that is radiated propagates out to infinity. Instead, in the plasma we find that as the string approaches the horizon it coils on top of itself over and over again with  $\rho$  tending to a finite  $\rho(1)$  at the horizon. This indicates that the energy deposited in the plasma (which can be thought of as having been left behind or radiated by the rotating quark) only spreads outwards to some finite radius. In the drag-dominated regime, where  $\rho(1) = \ell$ , the quark leaves a wake behind along its trajectory, as for linear motion at constant velocity. In the acceleration-dominated regime, where  $\rho(1) > \ell$ , the deposited energy spreads outwards, but not to infinity. So, in the acceleration-dominated regime  $dE/dt$  is as if the rotating quark were emitting synchrotron radiation in vacuum, but the behavior of the energy that the quark deposits in the plasma is different than that of synchrotron radiation in vacuum.

One way to gain further insight would be to calculate the stress-energy tensor for the plasma being stirred by the rotating quark. For the case of a quark in linear motion, the work of Refs. [22] has illuminated how the strongly coupled plasma carries the energy lost by the moving quark. By doing such a calculation for a rotating quark stirring the strongly coupled plasma, we could see whether in the acceleration-dominated regime the stress energy tensor in the region  $\rho < \rho(1)$  takes on the characteristic form expected for synchrotron radiation, with a pulse of energy density passing any distant point once every  $2\pi/\omega$  in time, and with these pulses having a width  $\sim L/\gamma^3$  that narrows with increasing  $v$ . We have seen in Section 2.3 that  $\rho(1)$  tends to a constant if  $\omega$  is increased at constant  $\gamma$  while  $\rho(1)$  increases without bound if  $\gamma$  is increased at constant  $\omega$ . This suggests that the distance that the energy left behind by the rotating quark spreads before it thermalizes is controlled by the width of the synchrotron radiation pulses, not by the time between pulses. This speculation could be tested via a calculation of the stress energy tensor, which we leave to future work.

### 3.3 Where the calculation breaks down

The calculation of  $dE/dt$  in (3.6) for a quark moving in a straight line with constant velocity is known to break down at sufficiently large velocity for quarks with finite mass  $M$ . We can give our test quarks finite mass by putting the D3-brane on which they live at  $u = \Lambda$  with  $\Lambda$  finite and

$\Lambda \gg 1$ , yielding quarks with mass

$$M = \frac{\sqrt{\lambda} T \Lambda}{2}. \quad (3.16)$$

(This is equivalent, for our purpose, to the more sophisticated approach [23] of introducing a D7-brane that fills the part of the AdS space with  $u > \Lambda$ .) Then, the calculation of the trailing string (2.30) and the associated linear drag (3.6) breaks down when the worldsheet horizon located at  $u = u_c^{\text{linear}} = (1 - v^2)^{-1/4}$  reaches  $\Lambda$  [13]. One way to see that something must go wrong is to realize that if (2.30) were valid when  $v$  is so large that  $u_c^{\text{linear}} > \Lambda$  then the speed of the quark itself, at the D3-brane, would exceed that of light. Casalderrey-Solana and Teaney provided an equivalent and more physical understanding of what breaks down by noting that at this velocity the force required to keep the quark moving with this velocity becomes so great that the production of pairs of quarks and antiquarks with mass  $M$  becomes unsuppressed [13].<sup>5</sup> By the same argument, our calculation breaks down when  $\Pi$  gets so large that  $u_c = \Lambda$ . Upon noting from (2.24) that at large  $\Pi$  we have  $u_c \simeq \sqrt{\Pi \mathbf{w}}$ , this means that our calculation breaks down when  $\Pi \mathbf{w} = \Lambda^2$ .

In Fig. 5 we plot  $\Pi \mathbf{w} = \Lambda^2$  as a curve in the  $(\mathbf{w}, \gamma)$ -plane for  $\Lambda = \sqrt{10}$  and for  $\Lambda = 10$ . Our classical calculation is valid below this curve. As  $\Lambda$  increases, the curve sweeps upward and to the right. In Fig. 5 we also plot the criterion (3.14), namely  $\mathbf{w} = \gamma^{-3/2}$ . Below this curve, we have found that the energy loss  $dE/dt$  is given by the linear drag result (3.9); above this curve, we have found that  $dE/dt$  is given by the vacuum radiation result (3.13). We see that there is a large region of the  $(\mathbf{w}, \gamma)$ -plane in which our calculation is valid and the vacuum radiation result is obtained. For example, for any fixed  $v$  we can pick a  $\Lambda$  such that upon increasing  $\mathbf{w}$  the acceleration dominated regime (3.14), where  $\Pi$  is given by (3.13), is reached long before the calculation breaks down at  $u_c = \Lambda$ . However, if we first take the  $\omega \rightarrow 0$  limit at fixed  $v$ , and then study the result as a function of increasing  $v$ , we recover the previously known result for when the linear drag calculation breaks down. So, at any fixed  $\Lambda$  there is always a (perhaps very small) value of  $\mathbf{w}$  below which no acceleration-dominated regime exists with  $u_c < \Lambda$ . The shape of the red curves in Fig. 5 can easily be understood: at small  $v$ , we see from (3.13) that  $\Pi \mathbf{w} = \text{constant}$  corresponds to  $\mathbf{w} \propto 1/v$ ; at larger  $v$  but where (3.13) still applies, we find  $\mathbf{w} \propto \gamma^{-2}$ ; at some still larger  $v$ , therefore, the red curve must cross the  $\mathbf{w} = \gamma^{-3/2}$  curve; beyond this crossover region, once (3.9) applies,  $\Pi \mathbf{w} = \text{constant}$  corresponds to a constant  $\gamma$ , independent of  $\mathbf{w}$ , and the red curve becomes vertical.

## 4. Speculations About Linear Motion

We have given our conclusions in Section 3.2, and described the regime in which our calculation is valid in Section 3.3. In this Section, we speculate about possible implications of our results for quarks moving in a straight line.

Consider a quark moving in a straight line at a constant speed  $v$ . This means that there is an external force acting on it, and the external force is doing work at a rate  $dE/dt|_{\text{linear drag}}$  given by (3.6). Now, suppose we turn the external force off. The quark will decelerate due to the drag

---

<sup>5</sup>At the same velocity, the screening length characterizing the potential between a moving quark and antiquark becomes shorter than the quark Compton wavelength [8].

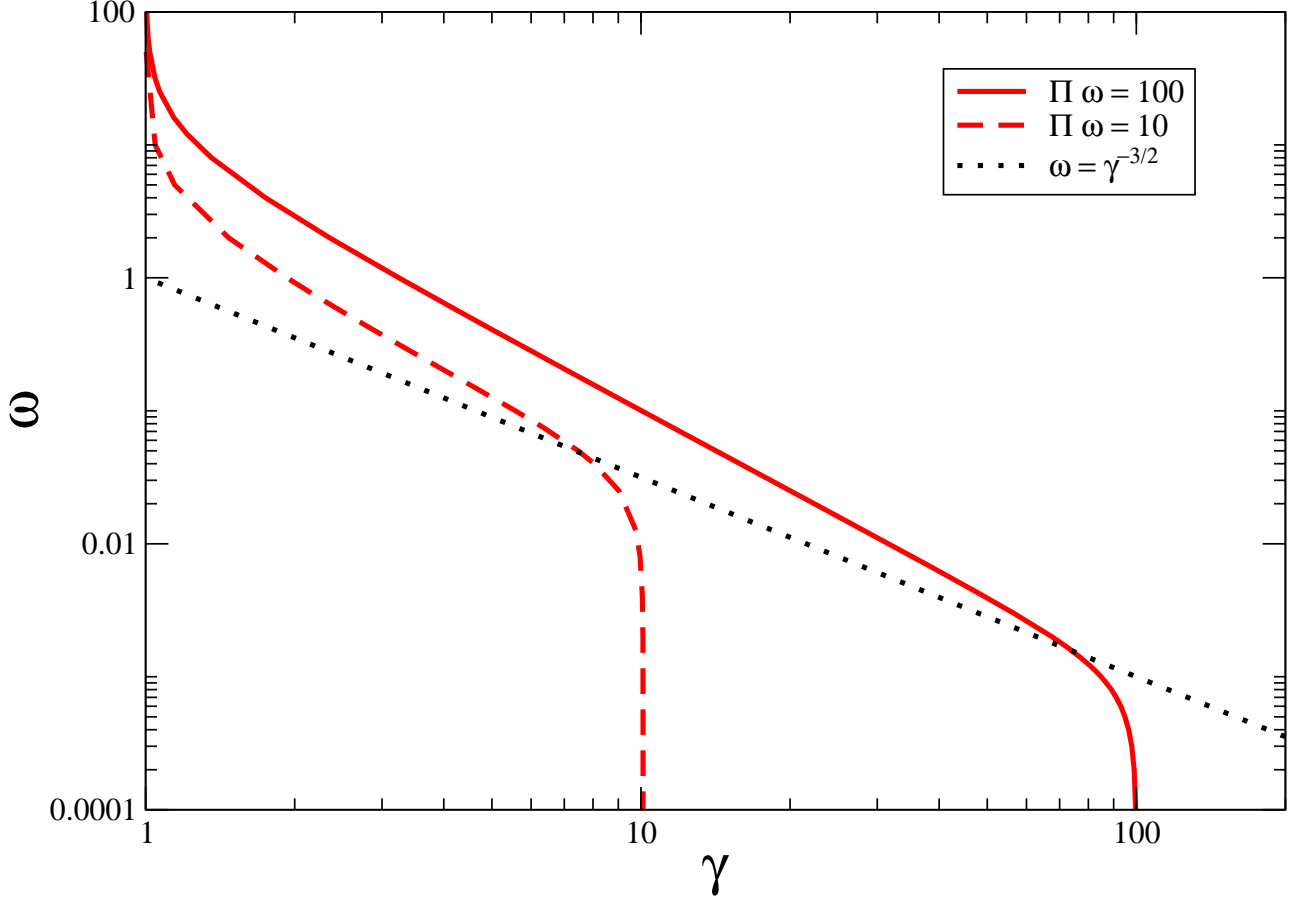


**Figure 5:** Regime of validity of our classical worldsheet calculation in the  $(\omega, \gamma)$ -plane as a function of quark mass. The calculation is valid for  $\Pi\omega < \Lambda^2$ , meaning below the red solid (dashed) curve for  $\Lambda = 10$  ( $\sqrt{10}$ ). The red curve sweeps upward and to the right as the quark mass  $M$ , given in (3.16), is increased and encompasses the whole plane as  $M \rightarrow \infty$ . The energy loss  $dE/dt$  is as for linear drag below the dotted line and as for radiation in vacuum above the dotted line. Noting in particular the smallness of the quark masses chosen in the plot and the log-scale used on the vertical axis, we see that there is a large region of parameter space in which the classical calculation is valid and the energy loss is as for acceleration-induced radiation in vacuum.

force. Let us calculate  $dE/dt|_{\text{vacuum radiation}}$  as if the quark were decelerating with this deceleration in vacuum. For  $\vec{a}$  in the same direction as  $\vec{v}$ , Mikhailov's result (3.10) becomes

$$\left. \frac{dE}{dt} \right|_{\text{vacuum radiation}} = \frac{\sqrt{\lambda}}{2\pi} \frac{a^2}{(1-v^2)^3} = \frac{\sqrt{\lambda}}{2\pi} \frac{1}{M^2} \left( \frac{dp}{dt} \right)^2, \quad (4.1)$$

where we have used  $p = M\gamma v$ .<sup>6</sup> At least initially,  $dp/dt$  will be that due to the drag force, namely [11,

<sup>6</sup>The corrections to Mikhailov's result at finite  $M$  due to the fact that the quarks have a nonzero Compton wavelength have been explored in Ref. [24]. We shall always assume that  $\Lambda$  is large enough that these corrections can be neglected.

12]

$$\frac{dp}{dt} = -\frac{\pi}{2}\sqrt{\lambda}T^2\frac{p}{M}. \quad (4.2)$$

We now see that the condition that  $dE/dt$  due to the vacuum radiation (4.1) caused by the drag-induced deceleration (4.2) be less than  $dE/dt$  due to the drag itself, (3.6), simplifies considerably and becomes just

$$\sqrt{\gamma} \ll \sqrt{\gamma_0} \equiv \frac{2M}{\sqrt{\lambda}T} = \Lambda, \quad (4.3)$$

where we have used (3.16). Remarkably, this is the same  $\gamma$  at which the classical worldsheet calculation breaks down, as we discussed in Section 3.3. So, for the case of linear motion, just at the velocity where the quark is about to enter an acceleration-dominated regime (by which we mean a regime in which, if the force moving the quark at constant velocity is turned off, the energy loss  $dE/dt|_{\text{vacuum radiation}}$  caused by the drag-induced deceleration would dominate over the energy loss due to the drag force itself) the calculation breaks down. In our calculation of a rotating quark, in contrast, we have found that the acceleration-dominated regime sets in long before the calculation breaks down. And, we have furthermore found that in this acceleration-dominated regime  $dE/dt$  turns out to be just as if the accelerating quark were radiating in vacuum, even though it is accelerating in a strongly coupled plasma.

Returning to the linear motion that we are focussing on in this Section, once the external force is turned off, the motion of a quark that initially has a large momentum in a direction that we shall term longitudinal can be described by the Langevin equations [25]

$$\frac{dp_L}{dt} = \xi_L(t) - \mu(p_L)p_L, \quad (4.4)$$

$$\frac{dp_i}{dt} = \xi_i(t) \quad (4.5)$$

with

$$\langle \xi_L(t)\xi_L(t') \rangle = \kappa_L(p_L)\delta(t-t') \quad (4.6)$$

$$\langle \xi_i(t)\xi_j(t') \rangle = \kappa_T(p_L)\delta_{ij}\delta(t-t'), \quad (4.7)$$

where  $p_L$  and  $p_i$  are the longitudinal and transverse momentum of the particle, respectively. Henceforth, we shall denote  $p_L$  by  $p$ .  $\xi_L$  and  $\xi_T$  are random fluctuating forces in the longitudinal and transverse directions.  $\langle \dots \rangle$  denotes the medium average. In general,  $\mu$ ,  $\kappa_T$  and  $\kappa_L$  will depend on  $p$ , but in  $\mathcal{N} = 4$  SYM theory in the regime (4.3) they are given by [11, 12, 14, 15, 13]

$$\mu = \frac{\pi}{2}\sqrt{\lambda}\frac{T^2}{M}, \quad \kappa_T = \pi\sqrt{\lambda}T^3\sqrt{\gamma}, \quad \kappa_L = \pi\sqrt{\lambda}T^3\gamma^{5/2}. \quad (4.8)$$

The calculations that lead to (4.8) are built upon the validity of the trailing string solution (2.30) as the description in the gravity dual of the quark moving at constant velocity, and so are valid only in the regime (4.3). However, when the velocity reaches the point at which  $\gamma \sim \gamma_0$  and (4.8)



therefore breaks down, there is no sign that the Langevin description (4.4-4.7) itself is breaking down. To see this, note that the solution of (4.4) is given by

$$p(t) = \int_0^t dt' e^{\mu(t'-t)} \xi_L(t') + p(0)e^{-\mu t} , \quad (4.9)$$

where we have assumed that  $\mu$  is  $p$ -independent and hence  $t$ -independent. From this solution we find that

$$\langle (\delta p)^2(t) \rangle = \frac{\kappa_L}{2\mu} (1 - e^{-2\mu t}) \quad (4.10)$$

which means that as long as  $t$  is not  $\ll 1/\mu$  we have

$$\langle (\delta p)^2(t) \rangle = \frac{\kappa_L}{2\mu} . \quad (4.11)$$

The Langevin description breaks down if the fluctuations (4.11) become large compared to  $p = M\gamma v$ . We can now see that while (4.8) is valid,

$$\frac{\langle (\delta p)^2(t) \rangle}{M^2 \gamma^2 v^2} = \frac{\sqrt{\gamma} T}{v^2 M} . \quad (4.12)$$

According to (4.3), (4.8) ceases to be valid at the velocity where  $\sqrt{\gamma} \sim \sqrt{\gamma_0}$ . But, at this velocity the right-hand side of (4.12) is  $\sim 1/\sqrt{\lambda}$ , meaning that it is parametrically small. So, at the velocity at which the trailing string description and hence the calculation of (4.8) breaks down, the Langevin description remains sound.

So far, we have described facts, not speculations.

We now speculate that a quark moving in a straight line with  $\gamma > \gamma_0$  is in a regime in which the Langevin description continues to be valid but the energy loss  $dE/dt$  is dominated by the radiation induced by the acceleration due to the fluctuating forces  $\xi_L$  and  $\xi_i$  in the Langevin description. And, inspired by our results for the rotating quark, we further speculate that this  $dE/dt$  is as if the accelerating quark were radiating in vacuum, namely

$$\left. \frac{dE}{dt} \right|_{\text{vacuum radiation}} = \frac{\sqrt{\lambda}}{2\pi M^2} \left( F_{\parallel}^2 + \gamma^2 \vec{F}_{\perp}^2 \right) , \quad (4.13)$$

where  $F_{\parallel}^2$  receives contributions from drag and from the fluctuating forces while  $F_{\perp}^2$  is due to the fluctuating forces alone. Near  $\gamma \sim \gamma_0$ , where (4.8) may still be a qualitative guide, perhaps the ratio of the contribution of the fluctuating forces to  $F_{\parallel}^2$  and  $F_{\perp}^2$  is of order  $\gamma^2$ . If so, then the two terms on the right-hand side of (4.13) make comparable contributions. It would be interesting to determine whether the  $\gamma^2 F_{\perp}^2$  term dominates when  $\gamma \gg \gamma_0$ , as is the case in a weakly coupled plasma.

We can now clearly see the significant advantage offered by the analysis of the rotating quark. In that situation, the onset of the acceleration-dominated regime occurs when the analogue of (4.3) is satisfied, meaning that we can do a reliable calculation. Upon so doing, we reached the conclusions described in Section 3, and in particular discovered that the energy loss in the acceleration-dominated regime is as if the quark were in vacuum.

## Acknowledgments

We acknowledge helpful conversations with Christiana Athanasiou, Tom Faulkner, Misha Stephanov and Laurence Yaffe. KBF is supported in part by Shahrood University of Technology research grant No. 24015 and by CERN. HL is supported in part by the A. P. Sloan Foundation and the U.S. Department of Energy (DOE) OJI program. This research was supported in part by the DOE Offices of Nuclear and High Energy Physics under grants #DE-FG02-94ER40818 and #DE-FG02-05ER41360.

## References

- [1] For reviews, see R. Baier, D. Schiff and B. G. Zakharov, *Ann. Rev. Nucl. Part. Sci.* **50**, 37 (2000) [arXiv:hep-ph/0002198]; R. Baier, *Nucl. Phys. A* **715**, 209 (2003) [arXiv:hep-ph/0209038]; A. Kovner and U. A. Wiedemann, arXiv:hep-ph/0304151; M. Gyulassy, I. Vitev, X. N. Wang and B. W. Zhang, arXiv:nucl-th/0302077; P. Jacobs and X. N. Wang, *Prog. Part. Nucl. Phys.* **54**, 443 (2005) [arXiv:hep-ph/0405125]; J. Casalderrey-Solana and C. A. Salgado, arXiv:0712.3443 [hep-ph].
- [2] K. Adcox *et al.* [PHENIX Collaboration], *Nucl. Phys. A* **757**, 184 (2005) [arXiv:nucl-ex/0410003]; B. B. Back *et al.* [PHOBOS Collaboration], *Nucl. Phys. A* **757**, 28 (2005) [arXiv:nucl-ex/0410022]; I. Arsene *et al.* [BRAHMS Collaboration]; *Nucl. Phys. A* **757**, 1 (2005) [arXiv:nucl-ex/0410020]; J. Adams *et al.* [STAR Collaboration], *Nucl. Phys. A* **757**, 102 (2005) [arXiv:nucl-ex/0501009].
- [3] F. Carminati *et al.* [ALICE Collaboration], *J. Phys. G* **30**, 1517 (2004); B. Alessandro *et al.* [ALICE Collaboration], *J. Phys. G* **32**, 1295 (2006); D. d'Enterria *et al.* [CMS Collaboration], *J. Phys. G* **34**, 2307 (2007); H. Takai, [for the ATLAS Collaboration] *Eur. Phys. J. C* **34**, S307 (2004).
- [4] J. Casalderrey-Solana, E. V. Shuryak and D. Teaney, *J. Phys. Conf. Ser.* **27** (2005) 22 [*Nucl. Phys. A* **774** (2006) 577] [arXiv:hep-ph/0411315].
- [5] J. M. Maldacena, *Adv. Theor. Math. Phys.* **2**, 231 (1998) [*Int. J. Theor. Phys.* **38**, 1113 (1999)] [arXiv:hep-th/9711200]; E. Witten, *Adv. Theor. Math. Phys.* **2**, 253 (1998) [arXiv:hep-th/9802150]; S. S. Gubser, I. R. Klebanov and A. M. Polyakov, *Phys. Lett. B* **428**, 105 (1998) [arXiv:hep-th/9802109]; O. Aharony, S. S. Gubser, J. M. Maldacena, H. Ooguri and Y. Oz, *Phys. Rept.* **323**, 183 (2000) [arXiv:hep-th/9905111].
- [6] B. G. Zakharov, *JETP Lett.* **65**, 615 (1997) [arXiv:hep-ph/9704255]; U. A. Wiedemann, *Nucl. Phys. B* **588**, 303 (2000) [arXiv:hep-ph/0005129].
- [7] H. Liu, K. Rajagopal and U. A. Wiedemann, *Phys. Rev. Lett.* **97**, 182301 (2006) [arXiv:hep-ph/0605178].
- [8] H. Liu, K. Rajagopal and U. A. Wiedemann, *JHEP* **0703** (2007) 066 [arXiv:hep-ph/0612168].
- [9] Y. Hatta, E. Iancu and A. H. Mueller, *JHEP* **0801**, 063 (2008) [arXiv:0710.5297 [hep-th]].
- [10] D. M. Hofman and J. Maldacena, *JHEP* **0805**, 012 (2008) [arXiv:0803.1467 [hep-th]].

- [11] C. P. Herzog, A. Karch, P. Kovtun, C. Kozcaz and L. G. Yaffe, JHEP **0607** (2006) 013 [arXiv:hep-th/0605158].
- [12] S. S. Gubser, Phys. Rev. D **74**, 126005 (2006) [arXiv:hep-th/0605182].
- [13] J. Casalderrey-Solana and D. Teaney, JHEP **0704**, 039 (2007) [arXiv:hep-th/0701123].
- [14] J. Casalderrey-Solana and D. Teaney, Phys. Rev. D **74**, 085012 (2006) [arXiv:hep-ph/0605199].
- [15] S. S. Gubser, Nucl. Phys. B **790**, 175 (2008) [arXiv:hep-th/0612143].
- [16] K. Peeters, J. Sonnenschein and M. Zamaklar, Phys. Rev. D **74** (2006) 106008 [arXiv:hep-th/0606195].
- [17] P. Burikham and J. Li, JHEP **0703** (2007) 067 [arXiv:hep-ph/0701259].
- [18] O. Antipin, P. Burikham and J. Li, JHEP **0706** (2007) 046 [arXiv:hep-ph/0703105].
- [19] F. Dominguez, C. Marquet, A. H. Mueller, B. Wu and B. W. Xiao, arXiv:0803.3234 [nucl-th].
- [20] A. Mikhailov, arXiv:hep-th/0305196.
- [21] A. Liénard, L'Éclairage Électrique **16** (1898) 5.
- [22] J. J. Friess, S. S. Gubser, G. Michalogiorgakis and S. S. Pufu, Phys. Rev. D **75**, 106003 (2007) [arXiv:hep-th/0607022]; S. S. Gubser, S. S. Pufu and A. Yarom, JHEP **0709**, 108 (2007) [arXiv:0706.0213 [hep-th]]; S. S. Gubser, S. S. Pufu and A. Yarom, Phys. Rev. Lett. **100**, 012301 (2008) [arXiv:0706.4307 [hep-th]]; P. M. Chesler and L. G. Yaffe, Phys. Rev. Lett. **99**, 152001 (2007) [arXiv:0706.0368 [hep-th]]; P. M. Chesler and L. G. Yaffe, arXiv:0712.0050 [hep-th].
- [23] A. Karch and E. Katz, JHEP **0206**, 043 (2002) [arXiv:hep-th/0205236].
- [24] M. Chernicoff and A. Guijosa, JHEP **0806**, 005 (2008) [arXiv:0803.3070 [hep-th]].
- [25] G. D. Moore and D. Teaney, Phys. Rev. C **71**, 064904 (2005) [arXiv:hep-ph/0412346].